A SPH Model with Open Relaxation Boundary for Wave Generation and Absorption

Guixun Zhu, Jason Hughes, Siming Zheng and Deborah Greaves
School of Engineering, Computing and Mathematics, University of Plymouth, Drake Circus, Plymouth PL4 8AA, UK

ABSTRACT

In this paper, a numerical wave tank with open relaxation boundary for wave simulation is presented under the framework of weakly compressible Smoothed Particle Hydrodynamics (SPH). The open relaxation boundary consists of open boundaries and relaxation particles. A relaxation function is applied for the relaxation particles which are placed between the inflow/outflow zone and the fluid domain. Open particles lie in the inflow/outflow regions to avoid kernel truncation. The open particles and relaxation particles can be created and deleted depending on the fluid motion around the open boundaries, and the properties of these particles can be obtained from theoretical resolution or by extrapolating within the domain. The model is validated by simulating a 2^{nd} Stokes wave and wave runup on a beach. The results demonstrate that the present SPH model with open relaxation boundary works well in wave generation and absorption.

KEY WORDS: Smoothed Particle Hydrodynamics; Open Boundary; Wave Simulation.

INTRODUCTION

Smoothed particle hydrodynamics (SPH) is a numerical method originally developed for astrophysical modeling (Gingold and Monaghan, Lucy, 1977) and later adapted for free-surface flow simulations (Monaghan, 1994). In recent years, the application of SPH to engineering problems has had a steady increase. SPH is a Lagrangian and mesh-less method, which uses a series of particles carrying physical properties to describe computational fluid dynamics (Liu and Liu, 2010). The Lagrangian reference frame of SPH makes it useful in solving problems with large deformations and complex free surfaces (Ye et al., 2019).

In this regard, SPH has been successfully applied to a number of free-surface problems that involve wave simulation and wave structure interaction (Liu and Zhang, 2019, Gotoh etal., 2018). Bouscasse et al. (2013) described a complete algorithm able to compute fully coupled viscous water wave and solid interactions using a $\delta-$SPH solver. Altomare et al (2017) presented a fully comprehensive SPH implementation of wave generation and active wave absorption for long-crested monochromatic and random waves using a piston-type wavemaker. Crespo et al. (2017) applied a GPU–accelerated SPH code (DualSPHysics) to simulate wave interaction with a floating offshore moored OWC device. It was demonstrated that the model was able to reproduce the water surface correctly inside the chamber. Meringolo et al. (2018) presented an analysis of the variation with time of mechanical and internal energies during wave generation, propagation and absorption. Zhang et al. (2018) applied SPH in the simulations of an oscillating wave surge converter (OWSC). The results demonstrated that the active power of a land hinged OWSC strongly depends on both the power take off damping coefficients and the wave periods. He et al. (2020) presented a numerical investigation of the solitary wave breaking over a slope by using a enhanced SPH model. Brito et al. (2020) presented a SPH model with nonlinear mechanical constraints for OWSC and analyzed the effect of the flap inertia.

Inflow and outflow boundary conditions can limit the size of the computational domain to a region of interest. An open boundary near inflow and outflow boundary needs some special attention to ensure reliable results. The topic of open boundaries in SPH was previously investigated. A characteristic-based non-reflecting open boundary formulation for internal flows has been proposed by Lastiwka et al (2009). Federico et al. (2012) presented an implementation of open boundary conditions for free-surface flow. Buffer layers are created at inflow/outflow regions. Physical variables of outflow buffer particles are frozen with the exception of their positions that evolve according to the velocities. Ferrand et al. (2017) introduced a different approach based on the generalization of the semi-analytical boundary conditions method to impose unsteady open boundaries. Tafuni et al (2018) proposed a versatile algorithm by using the higher order interpolation scheme of Liu and Liu. (2010) to extrapolate the property of buffer particles. Ni et al. (2018) presented a wave generation and absorption technique with non-reflective open boundaries in 2018, which was capable of generating multiple types of waves, including solitary waves, linear and second-order regular waves. In 2019, Tim et al. (2019) also introduced the implementation of non-linear wave generation and absorption by open boundaries in DualSPHysics. The target wave was accurately produce by considering the inlet and outlet velocity correction. Relaxation zone is a numerical method in which the velocity

and water volume of the particles or grid is controlled by a relaxation function in wave generation domain. Relaxation zone method has been added to OpenFOAM Library (Jacobsen et al,2012) and is widely used for engineering problems (Chen et al., 2014, Vyzikas et al., 2017 and Hu et al., 2020). Relaxation zone method has also been introduced in SPH (Ni et al., 2013), and is extended to couple the Dual-SPHysics model to the wave propagation model SWASH (Altomare et al., 2018). The performance of relaxation zone depends on the hyperbolic function and the width of the relaxation zone. Moreover, Tsuruta et al (2021) presented a novel wave boundary model, namely Wavy Interface model, which is designed to omit a usual tuning process by keeping the desired wave front through generation/removal of the particles around the free surface. This method , which can considerable reduce CPU time, still uses open boundary to generate wave. He et al. (2021) derive a new formulae for the precise descent of an arbitrary-geometry plunger to produce solitary wave. However, this approach does not seem to reduce the computational effort and can only be used to generate isolated waves.

This research aims to develop a SPH model for wave generation and absorption by combining open boundary and relaxation zone. Relaxation zone is used to generate and absorb waves, while open boundary is imposed to allow wave tank to be short, and hence reduce the computational cost of simulation. The remainder of this paper is organized as follows. The SPH model and the open relaxation boundary are described in Section 2 and Section 3. Validation of the present model, including wave simulation and wave runup on a beach, is described in Section 4. Finally, conclusions are drawn in Section 5.

SPH MODEL

In this study, the flow is assumed to be viscous, weakly–compressible, and adiabatic. The adopted governing equations consist of the Navier–Stokes equations in the Lagrange framework:

$$\begin{cases} \frac{\mathrm{d}\boldsymbol{u}}{\mathrm{d}t} = -\frac{1}{\rho}\nabla P + \boldsymbol{F}_\alpha + \boldsymbol{g}, \\ \frac{\mathrm{d}\rho}{\mathrm{d}t} = -\rho\nabla\cdot\boldsymbol{u}, \\ \frac{\mathrm{d}\boldsymbol{r}}{\mathrm{d}t} = \boldsymbol{u}, \end{cases} \tag{1}$$

where ρ, ρ_0, $\boldsymbol{u}$, t, $\boldsymbol{r}$ and P denote the instant density, initial density, velocity vector, time, position vector and pressure, respectively. $\boldsymbol{F}_\alpha$ is the viscosity term and $\boldsymbol{g}$ represents the gravitational acceleration. The governing equation can be discretized by an SPH approximation. The discrete pressure gradient can be written as:

$$-\frac{1}{\rho_i}\nabla P_i = -\frac{1}{\rho_i}\sum_j (P_j + P_i)\cdot W_{ij}^{'} V_j, \tag{2}$$

where $W_{ij} = W(r_i - r_j, h)$ is the kernel function (Gauss kernel is used in this paper), $h = 1.2$ is the smoothing length defining the influence region. Subscripts i and j denote the particle index. V_j is the volume of the particle ($V_j = m_j/\rho_j$, m denotes mass).
The artificial viscosity term can be added to the momentum equation to produce bulk and shear viscosity and also to stabilize the scheme as follows

$$F_\alpha = \sum_j \alpha hc \frac{(\boldsymbol{u}_j - \boldsymbol{u}_i)\cdot(\boldsymbol{r}_j - \boldsymbol{r}_i)}{|\boldsymbol{r}_j - \boldsymbol{r}_i|^2}\cdot W_{ij}^{'} V_j. \tag{3}$$

where u_i is the velocity of particle i. Furthermore, the relationship between the artificial viscous coefficient α ($\alpha = 0.001$ in this paper) and the physical kinematic viscosity υ is

$$\upsilon = \frac{\alpha hc}{2(dim + 2)}, \tag{4}$$

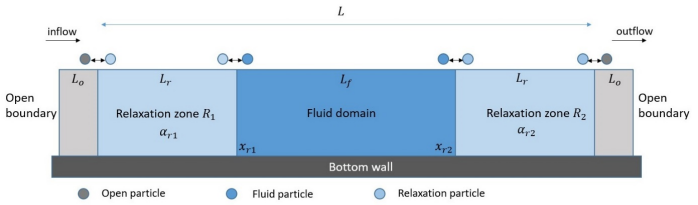

Fig. 1 Sketch of open relaxation boundary.

where *dim* is the number of spatial dimensions.
The velocity divergence can be discretized

$$-\rho_i\nabla\cdot\boldsymbol{u}_i = -\sum_j (\boldsymbol{u}_j - \boldsymbol{u}_i)\cdot W_{ij}^{'} V_j, \tag{5}$$

Spurious numerical oscillations generally exist in the pressure and density fields for traditional weakly compressible SPH. One of the popular methods to overcome the problem is the δ–SPH model (Antuono et al., 2012), in which a diffusive term is added to the continuity equation to remove the spurious high–frequency oscillations. This method is employed in the present study with the added diffusive term expressed as

$$\delta hc \sum_j \Psi_{ij}\cdot\nabla_i W_{ij} V_j, \tag{6}$$

where $\delta = 0.1$ (Marrone et al., 2011) for all the following cases and

$$\begin{cases} \Psi_{ij} = 2(\rho_j - \rho_i)\frac{\boldsymbol{r}_j - \boldsymbol{r}_i}{|\boldsymbol{r}_j - \boldsymbol{r}_i|^2} - (\langle\nabla\rho\rangle_i^L + \langle\nabla\rho\rangle_j^L), \\ \langle\nabla\rho\rangle_i^L = \sum_j(\rho_j - \rho_i)L_i W_{ij}^{'} V_j, \quad \text{where} \quad L_i = [\sum_j(\boldsymbol{r}_j - \boldsymbol{r}_i)\otimes W_{ij}^{'} V_j]^{-1} \end{cases} \tag{7}$$

where $\otimes$ denotes tensor product. Meanwhile, the fluid pressure is related to the density explicitly according to the concept of artificial compressibility. Then, the pressure is obtained through the equation of state as

$$P = (\rho - \rho_0)c^2, \tag{8}$$

where c is the numerical speed of sound, which is chosen following an analysis presented by Morris et al., (1997) to approximate an incompressible flow accurately. In the present simulation, a prediction–correction time–stepping scheme is applied to ensure second–order accuracy (Monaghan, 1989). Following Marrone et al., (2011), the present model uses the regular fixed ghost particles that are created to represent the solid boundary.

OPEN RELAXATION BOUNDARY

The open relaxation boundaries are implemented as open and relaxation particles zones. Physical quantities, such as velocity, surface height and pressure, can be applied to these particles. The imposed physical quantities can originate from wave theory or data from other numerical simulation results. The schematic in Fig. 1 briefly depicts the open relaxation boundary. Open particles zones are placed in the inflow/outflow regions to cover the truncated kernel area. The number of open particle layers is determined by the kernel function and compact support. In this work, each open particles zone consists of 4 layers of buffer particles. Relaxation particles are immediately followed by boundary particles for wave generation and absorption. A relaxation function is used in relaxation particles zones to ensure a smooth and stable flow field.
The position of each kind of particle is updated according to the velocity in the time integration method.The position is used as a basis to distinguish particle species. The variation of particle species obeys the following rules:

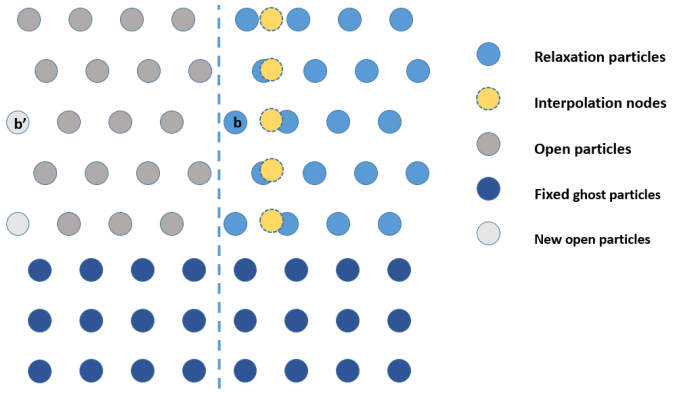

Fig. 2 Sketch of computational domain near inflow/outflow region.

1. As open particles cross the boundaries of the computational domain, they are removed from the domain.
2. Open particle (b) entering the relaxation region is transformed into relaxation particle and new open particle (b') is created in the open region. The vertical position of particle (b') is the same as particle b. And the horizontal position of particle (b') differs from particle (b) by four initial particle spacing, as shown in Fig. 2.
3. Relaxation particles and fluid particles are updated based on the updates of position.

All three types of particles have different treatment methods. Open particles apply velocity, surface height and pressure. For relaxation particles, we apply the horizontal velocity and use a relaxation function to ensure a smooth transition. The properties of the fluid particles are obtained by solving the governing equations. Here, we specifically introduce the processing methods for open particles and relaxation particles.

To obtain the properties of the open particles, interpolation nodes are used. Along the normal direction of the open boundary, the interpolation nodes are arranged one initial particle spacing away from the open boundary line as shown in Fig. 2. In the vicinity of the interpolation node, SPH interpolation does not give good results due to the presence of kernel truncation. For the interpolation nodes, the physical properties can be reconstructed by moving least square (MLS) reconstruction.

Suppose that $f(\boldsymbol{r})$ is the local pressure of velocity field function in the support domain of interpolation nodes. The approximation of $f(\boldsymbol{r})$ at the position of relaxation particles is denoted as $f^h(\boldsymbol{r})$. Then $f^h(\boldsymbol{r})$ can be calculated with the help of a basis as:

$$f^h(\boldsymbol{r}) = \sum_{i=1}^{m} q(\boldsymbol{r}_i)c(\boldsymbol{r}_i) = q^T(\boldsymbol{r})c(\boldsymbol{r}), \tag{9}$$

where $c(\boldsymbol{r})$ is the basis function and m is the term numbers of basis function. In this work, the quadratic basis is used as

$$q^T(\boldsymbol{r}) = [1, x, y, x^2, xy, y^2], m = 6. \tag{10}$$

$c(\boldsymbol{r})$ is the undetermined coefficients and can be expressed as

$$c(\boldsymbol{r}) = [c(r_1), c(r_2), ..., c(r_m)]. \tag{11}$$

Since pressure and velocity are interpolated here, $f^h(\boldsymbol{r})$ can denote the local pressure and velocity reconstruction field here and is influenced by the nearby relaxation particles. Thus, we can construct a function of weighted residual J:

$$J = \sum_{j=1}^{n} W_s(\boldsymbol{r}_j)(f^h(\boldsymbol{r}_j) - f(\boldsymbol{r}_j))^2 = \sum_{j=1}^{n} W_s(\boldsymbol{r}_j)[q^T(\boldsymbol{r}_j)c(\boldsymbol{r}_j) - f(\boldsymbol{r}_j))^2], \tag{12}$$

where $W_s(\boldsymbol{r})$ is a weight function and n is the number of relaxation particles inside the support domain of the weight function.

For an arbitrary relaxation particle, the value of $c(\boldsymbol{r})$ can be determined by the minimizing the weighted residual J

$$\frac{\partial J}{\partial c} = \boldsymbol{A}(\boldsymbol{r})c(\boldsymbol{r}) - \boldsymbol{B}(\boldsymbol{r})\boldsymbol{F} = 0, \tag{13}$$

where $\boldsymbol{A}(\boldsymbol{r})$ is given as

$$\boldsymbol{A}(\boldsymbol{r}) = \sum_{j=1}^{n} W_s(\boldsymbol{r}_j)q^T(\boldsymbol{r}_j)q(\boldsymbol{r}_j), \tag{14}$$

and $\boldsymbol{B}(\boldsymbol{r})$ is given as

$$\boldsymbol{B}(\boldsymbol{r}) = q^T(\boldsymbol{r})W_s(\boldsymbol{r}) = [q(\boldsymbol{r}_1)W_s(\boldsymbol{r}_1), q(\boldsymbol{r}_2)W_s(\boldsymbol{r}_2), ..., q(\boldsymbol{r}_n)W_s(\boldsymbol{r}_n)], \tag{15}$$

and $\boldsymbol{F}$ is field value

$$\boldsymbol{F} = [f_1, f_2, ..., f_n], \tag{16}$$

Solving for $c(\boldsymbol{r})$ from Eq. (13) and substituting it into Eq. (9) leads to

$$f^h(\boldsymbol{r}) = q^T(\boldsymbol{r})c(\boldsymbol{r}) = q^T(\boldsymbol{r})\boldsymbol{A}^{-1}(\boldsymbol{r})\boldsymbol{B}(\boldsymbol{r})\boldsymbol{F} = \Phi^T(\boldsymbol{r})\boldsymbol{F}, \tag{17}$$

where $\Phi^T(\boldsymbol{r})$ is the shape function. The first derivative of the field function is given as

$$f_i^h(\boldsymbol{r}) = \Phi_i^T(\boldsymbol{r})\boldsymbol{F} = (q_i^T(\boldsymbol{r})\boldsymbol{A}^{-1}(\boldsymbol{r})\boldsymbol{B}(\boldsymbol{r}) + q^T(\boldsymbol{r})\boldsymbol{A}_i^{-1}(\boldsymbol{r})\boldsymbol{B}(\boldsymbol{r}) + q^T(\boldsymbol{r})\boldsymbol{A}^{-1}(\boldsymbol{r})\boldsymbol{B}_i(\boldsymbol{r}))\boldsymbol{F}, \tag{18}$$

The pressure or velocity of open particles can be inferred from the interpolated nodes.

The open particles are perfectly connected to the relaxation particles for horizontal velocities by the use of relaxation equation. However, the pressure interface between these two kinds of particles still needs to be considered carefully. Radiation condition proposed by Orlanski (1976), works well as passive boundary, allowing disturbances to propagate out of the computational domain. The radiation condition is

$$\frac{\partial P}{\partial t} + C_w \frac{\partial P}{\partial \boldsymbol{n}} = 0, \tag{19}$$

where $C_w = \sqrt{gd}$ (d is free surface level), $\boldsymbol{n}$ is the vertical direction of open boundary. Thus, the pressure of open particles at now is calculated as:

$$p_o^{now} = p_o^{last} - C_w * t_0 \nabla p_o^{last}|_{\boldsymbol{n}}, \tag{20}$$

where $\nabla p_o^{last} = \nabla p_i^{last}$, o and i denote the vertical velocity, open boundaries and interpolation node. t_0 is the time step. Here, the vertical velocity is $v_o = v_i$ with the assumption of tangential radiation in Orlanski (1976). The horizontal velocity of the open particle is imposed based on the wave theory.In wave simulations, the free surface level in the open region is not constant. The free surface evolution is performed on the open boundary. The theoretical free surface height at each moment can be obtained based on wave theory. If the difference between the theoretical level and the SPH result is greater than one initial particle spacing, a layer of open particles will be added or removed.

Relaxation particles zones are implemented to generate wave and avoid reflection of waves in the computational domain. The reflection waves obviously contaminates the results. And the relaxation particles zone is

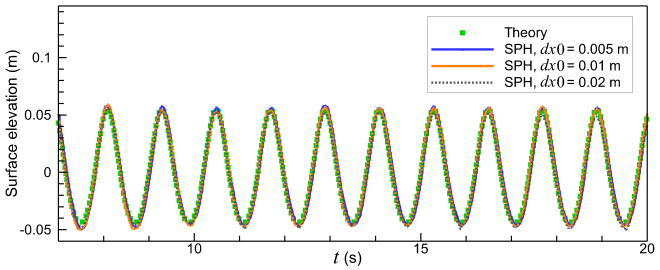

Fig. 3 Time series of the water surface elevation at the centre of the domain predicted by the SPH methods with three different resolutions, i.e., $dx0$ = 0.005 m, 0.01 m and 0.02 m, together with the theoretical solutions.

found to produce a continuities in the surface elevation between open particles zones and fluid zones.

The present relaxation technique is an extension to that of Mayer et al. (1998) and Jacobsen et al. (2012). A relaxation function

$$\alpha_r(x_i) = \begin{cases} 1.0 - \frac{\exp(\chi_{r1}^{\beta})-1}{\exp(1)-1}, & i \in r1, \\ 1.0 - \frac{\exp(\chi_{r1}^{\beta})-1}{\exp(1)-1}, & i \in r2, \end{cases} \tag{21}$$

is applied inside the relaxation zone in the following way

$$\phi = \alpha_r \phi_{sph} + (1-\alpha_r)\phi_{target}, \tag{22}$$

where ϕ represents horizontal velocity, β is 3.5, $\chi_{r1} = \frac{|x_i - x_{r1}|}{L_r}$ and $\chi_{r2} = \frac{|x_i - x_{r2}|}{L_r}$. $R1$ and $R2$ are relaxation particles zones as shown in Fig. 1. The definition of χ_r ensures that α_r is always 1 at the interface between fluid particles zone and the relaxation particles zones, and α_r is always 0 at the interface between open particles zones and the relaxation particles zones. The vertical velocity and pressure of the relaxation particles are calculated by solving the governing equation.

NUMERICAL RESULTS

In this section, the wave generation and absorption of 2^{nd} Stokes wave is conducted for present SPH numerical wave tank. Then, validated model is applied to simulate the regular wave runup on a beach.

Regular wave simulation

This section is to verify the performance of a SPH–based NWT with open relaxation boundary by comparing the numerical results with the analytical ones. A 2^{nd} Stokes wave (wave period T = 1.2 s, wave height H= 0.1 m and) is simulated for investigating the present model. A 2-D computational domain with water depth d = 0.5 m and length L = 6.03 m (three wave lengths)is used. The accuracy of wave propagation and absorption with open relaxation boundaries is now assessed by comparing SPH surface elevation.

Time series of the water surface elevation at the centre of the domain predicted by the SPH methods with three different resolutions are illustrated in Fig. 3. It is clear that the surface elevation is simulated with a very high accuracy. Both the wave crest and wave are reproduced excellently. For quantifying and better evaluating the comparison between the reference results, the mean average errors for amplitude MAE_a and phase MAE_p are used, which are calculated according to equations

$$MAE_a = \frac{1}{N_a}\sum \frac{|\eta_{extr}^{ref} - \eta_{extr}^{sph}|}{A}, \tag{23}$$

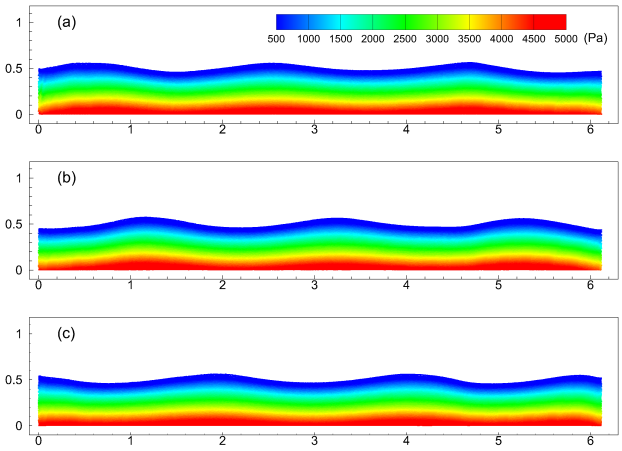

Fig. 4 Pressure field distribution of numerical wave tank at t= 13.7 s (a), 14.1 s (b) and 14.5 s (c).

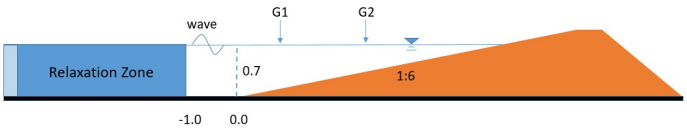

Fig. 5 Sketch of the numerical tests of regular wave runup on a beach.

$$MAE_p = \frac{1}{N_a}\sum \frac{|t_{extr}^{ref} - t_{extr}^{sph}|}{T}, \tag{24}$$

where $extr$ refers to the local extrema, A to the wave amplitude and N_a to the number of wave crest. ref and sph denote reference data (e.g., theory or experimental data) and SPH results, respectively. Numerical results for the two finer resolutions overlay one another and agree well with the analytical results, indicating that a convergent solution seems to be achieved with $dx0 \leq 0.01$ m. The calculated errors MAE_a and MAE_p for particle spacing 0.005 m are 1.3% and 1.9%. Fig. 4 shows a smooth pressure field near the open boundary. The results prove that the open relaxation boundary is capable of accurately reproducing the surface elevation and pressure field.

Wave runup on a beach

Wave runup on a beach is a common coastal hydrodynamic phenomenon. The wave shoaling leads to the increasing nonlinearity, which should be accurately simulated by a qualified hydrodynamic model. In this section, a regular wave runup case is modeled by the proposed numerical wave tank with a 1:6 slop beach. The water depth at the toe of the beach is 0.7 m, relaxation zone is 5.0 m and the open boundary wave generation is 1.0 m away from the toe, as shown in Fig. 5. Initial particle spacing is 0.01 m and time step is 0.0001 s. The regular wave height and period are 0.16 m and 2.0 s, respectively. Two wave gauges are deployed at x=1.02 m and x=2.81 m, following the experiment arrangement of Li et al. (2004). Satisfactory agreements are found in comparison between the numerical results and experimental data (Li et al., 2004) at two wave gauges in Fig. 6. Fig. 7 shows the pressure field. The pressure noise introduced by the open boundary can hardly be observed. Meanwhile, pressure oscillations from waves slamming slope do not affect the pressure distribution near the open boundary indicating the validity and reliability of the open relaxation boundary condition wave generation technique proposed in this paper.

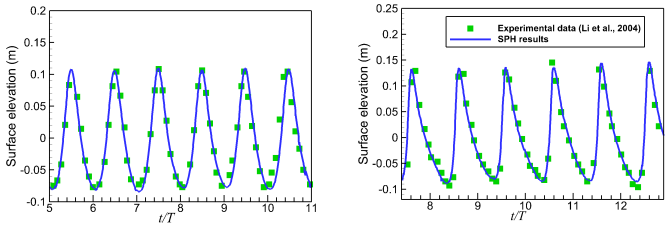

Fig. 6 The time evolution of the surface elevations: (a) wave gauge G1 at x=1.02 m, (b) wave gauge G2 at x = 2.81 m.

CONCLUSIONS AND DISCUSSION

In this paper, a novel framework has been proposed for simulating wave in SPH numerical wave tank with open relaxation boundary. The open relaxation boundary involves open zones and relaxation zones. The particles in open zone, called open particles, are used for avoiding kernel truncation at inflow/outflow region. Pressure and vertical velocity of the open particles are obtained by using the moving least square construction and radiation condition. The horizontal velocity of the open particles is imposed based on wave theory. A relaxation function is applied for relaxation particles for the horizontal velocity. The pressure and vertical velocity of relaxation particles are calculated by solving the governing equation. Accurate free surface evolution results can be obtained for 2^{nd} stokes wave case and wave runup on a beach. Meanwhile, smooth pressure field near the inflow/outflow region is obtained. The results demonstrate the capability of the present open relaxation boundary to model wave generation and absorption.

ACKNOWLEDGMENTS

Guixun Zhu was supported by the financial support from China Scholarship Council (Grant No. 201806060137). Siming Zheng gratefully acknowledges the support from the European Union funded Marine-I (2^{nd} phase) project (grant no. 05R18P02816), and Open Research Fund Program of State Key Laboratory of Hydroscience and Engineering, Tsinghua University (Grant No. sklhse-2021-E-02).

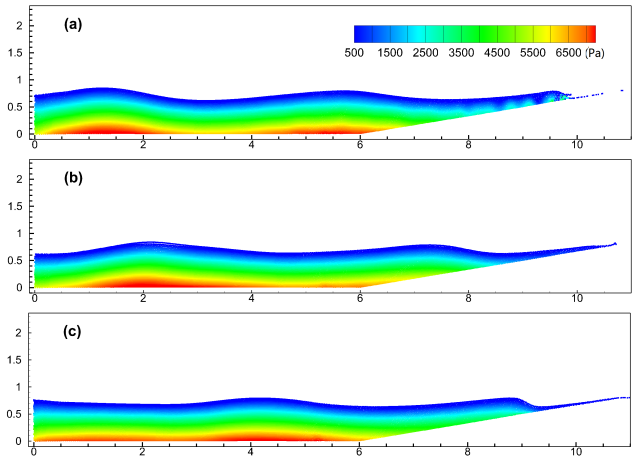

Fig. 7 Pressure field distribution of regular wave runup on a beach at t/T= 6.35 s (a), 6.6 s (b) and 6.85 s (c).

REFERENCES

Altomare, C, Domínguez, J, Crespo, A, González-Cao, J, Suzuki, T, Gómez-Gesteira, M and Troch, P. (2017). "Long-crested wave generation and absorption for SPH-based DualSPHysics model", *Coastal Engineering*, Vol. 27, pp. 37–54.

Antuono, M, Colagrossi, A and Marrone, S. (2012). "Numerical diffusive terms in weakly–compressible SPH schemes", *Computer Physics Communications*, Vol. 183, pp. 2570–2580.

Antuono, M, Colagrossi, A. Marrone, S and Lugni, c. (2012). "Propagation of gravity waves through an SPH scheme with numerical diffusive terms", *Computer Physics Communications*, Vol. 182, pp. 866–877.

Bouscasse, B, Colagrossi, A, Marrone, S and Antuono, M. (2013). "Nonlinear water wave interaction with floating bodies in SPH", *Computer Physics Communications*, Vol. 42, pp. 112–129.

Brito, M, Canelas, R, García-Feal, O, Domínguez, J, Crespo, A, Ferreira, R, Neves, M and Teixeira, L. (2020). "A numerical tool for modelling oscillating wave surge converter with nonlinear mechanical constraints", *Renewable Energy*, Vol. 146, pp. 2024–2043.

Chen, L, Zang, J, Hillis, A, Morgan, G and Plummer, A. (2014). "Numerical investigation of wave–structure interaction using OpenFOAM", *Ocean Engineering*, Vol. 88, pp. 91–109.

Crespo, A, Altomare, c, Domínguez, J, González-Cao, J and Gómez-Gesteira, M. (2017). "Towards simulating floating offshore oscillating water column converters with Smoothed Particle Hydrodynamics", *Coastal Engineering*, Vol. 126, pp. 11–26.

Federico, I, Marrone, S, Colagrossi, A, Aristodemo, F and Antuono, M. (2012). "Simulating 2D open-channel flows through an SPH model", *European Journal of Mechanics-B/Fluids*, Vol. 34, pp. 35–46.

Ferrand, M, Joly, A, Kassiotis, C, Violeau, D, Leroy, A, Morel, F, Rogers, B. (2017). "Unsteady open boundaries for SPH using semi-analytical conditions and Riemann solver in 2D", *Computer Physics Communications*, Vol. 210, pp. 29–44.

Gingold, R and Monaghan, J. (1977). "Smoothed particle hydrodynamics: theory and application to non-spherical stars", *Monthly notices of the royal astronomical society*, Vol. 181, pp. 375–389.

Gotoh, H, and Khayyer, A. (2018). "On the state-of-the-art of particle methods for coastal and ocean engineering", *Coastal Engineering Journal*, Vol. 60, pp. 79—103.

He, F, Zhang, H, Huang, C and Liu, M. (2020). "Numerical investigation of the solitary wave breaking over a slope by using the finite particle method", *Coastal Engineering*, Vol. 156, 103617.

He, M, Khayyer, A, Gao, X, Xu, W, and Liu, B. (2020). "Theoretical method for generating solitary waves using plunger-type wavemakers and its Smoothed Particle Hydrodynamics validation", *Applied Ocean Research*, Vol. 106, 102414.

Hu, Z, Yan, S, Greaves, D, Mai, T, Raby, A and Ma, Q. (2020). "Investigation of interaction between extreme waves and a moored FPSO using FNPT and CFD solvers", *Ocean Engineering*, Vol. 206, 107353.

Jacobsen, N, Fuhrman, D and Fredsøe, J. (2012). "A wave generation toolbox for the open-source CFD library: OpenFoam", *International Journal for numerical methods in fluids*, Vol. 70, pp. 1073–1088.

Lastiwka, M, Basa, M and Quinlan, N. (2009). "Permeable and non-reflecting boundary conditions in SPH", *International Journal for numerical methods in fluids*, Vol. 61, pp. 709–724.

Li, T, Troch, P and De Rouck, J. (2004). "Wave overtopping over a sea dike", *Journal of Computational Physics*, Vol. 198, pp. 686–726.

Liu, M and Zhang, Z. (2019). "Smoothed particle hydrodynamics (SPH) for modeling fluid-structure interactions", *Science China Physics, Mechanics & Astronomy*, Vol. 62, 984701.

Liu, M and Liu, G. (2010). "Smoothed particle hydrodynamics (SPH): an overview and recent developments", *Archives of computational methods in engineering*, Vol. 17, pp. 25–76.

Lucy, B. (1977). "A numerical approach to the testing of the fission hypothesis", *The astronomical journal*, Vol. 82, pp. 1013–1024.

Marrone, S, Antuono, M, Colagrossi, A, Colicchio, G, Le Touzé, D and Graziani, G. (2011). "δ-SPH model for simulating violent impact flows", *Computer Methods in Applied Mechanics and Engineering*, Vol. 200, pp. 1526–1542.

Mayer, S, Garapon, A and Sørensen, L. (1988). "A fractional step method for unsteady free-surface flow with applications to non-linear wave dynamics", *International Journal for Numerical Methods in Fluids*, Vol. 28, pp. 293–315.

Meringolo, D, Aristodemo, D and P. Veltri. (1988). "SPH numerical modeling of wave–perforated breakwater interaction", *Coastal Engineering*, Vol. 101, pp. 48–68.

Meringolo, D, Liu, Y, Wang, X and Colagrossi, A. (2018). "Energy balance during generation, propagation and absorption of gravity waves through the δ-LES-SPH model", *Coastal Engineering*, Vol. 140, pp. 355–370.

Monaghan, J. J. (1989). "On the Problem of Penetration in Particle Methods", *Journal of Computational Physics*, Vol. 82, pp. 1–15.

Monaghan, J. J. (1994). "Simulating Free Surface Flows with SPH", *Journal of Computational Physics*, Vol. 110, pp. 399–406.

Monaghan, J. J. (2005). "Smoothed particle hydrodynamics", *Reports on Progress in Physics*, Vol. 68, pp. 1703–1759.

Morris, J, Fox, P and Zhu, Y. (1997). "Modeling low Reynolds number incompressible flows using SPH", *Journal of computational physics*, Vol. 136, pp. 214–226.

Ni, X, Feng, W. (2013). "Numerical simulation of wave overtopping based on DualSPHysics", *Applied Mechanics and Materials*, Vol. 405, pp. 1463–1471.

Ni, X, Feng, W, Huang, S, Zhang, Y and Feng, X. (2018). "A SPH numerical wave flume with non-reflective open boundary conditions", *Ocean Engineering*, Vol. 163, pp. 483–501.

Orlanski, I. (1976). "A simple boundary condition for unbounded hyperbolic flows", *Journal of computational physics*, Vol. 21, pp. 251–269.

Tafuni, A, Dom´ınguez, J, Vacondio, R and Crespo, A. (2019). "A versatile algorithm for the treatment of open boundary conditions in smoothed particle hydrodynamics GPU models", *Computer Methods in Applied Mechanics and Engineering*, Vol. 342, pp. 604–624.

Tim, v, José M, d, Corrado, A, Angelantonio, T, Renato, V, Peter, T and Andreas, K. (2019). "Non-linear wave generation and absorption using open boundaries within DualSPHysics", *Computer Physics Communications*, Vol. 342, pp. 604–624.

Tsuruta, N, Khayyer, A, Gotoh, H, and Suzuki, K. (2021). "Development of Wavy Interface model for wave generation by the projection-based particle methods", *Coastal Engineering*, Vol. 165, pp. 103861.

Vyzikas, T, Deshoulières, S, Giroux, O, Barton, M and D. Greaves. (2017). "Numerical study of fixed Oscillating Water Column with RANS-type two-phase CFD model", *Renewable Energy*, Vol. 102, pp. 294–305.

Ye, T, Ding, y, Pan, D, Huang, c and Liu, M. (2019). "Smoothed particle hydrodynamics (SPH) for complex fluid flows: Recent developments in methodology and applications", *Physics of Fluids*, Vol. 31, 011301.

Zhang, D, Shi, Y, Huang, C, Si, Y, Huang, B and Li, W. (2018). "SPH method with applications of oscillating wave surge converter", *Ocean Engineering*, Vol. 152, pp. 273–285.